Chapter 7
Bioelectrochemical and Reversible Interconversion in the Proton/Hydrogen and Carbon Dioxide/Formate Redox Systems and Its Significance in Future Energy Systems

Yuki Kitazumi and Kenji Kano

7.1 Introduction

Energy is an integral part of human activities. The industrialization and growing population in the world require increasing amounts of energy. To a great extent, major economies of the present-day world rely on fossil fuels. Increasing consumption of fossil fuels is not environmentally friendly, since fossil fuels release greenhouse gases and other pollutants as major contributors to planet warming (European Commission 2003). These global energy problems could be solved by sourcing environmentally clean, cheap, and sustainable energy systems. The introduction of hydrogen (H_2) is considered as the universal vector for conveying renewable forms of energy and as an ultimate ideal sustainable non-pollutant fuel (Rand 2011; Ren et al. 2017; Sahaym and Norton 2008). The proposal to use H_2 as both an energy vector and an ultimate fuel has become known as hydrogen economy or hydrogen energy system in the present day (Fig. 7.1), though the term "hydrogen economy" was first used by J. O'Mara Bockris in 1970 at General Motors Technical Center (Abe et al. 2019). On the other hand, electrical energy is the most important, versatile, and useful of the secondary energy sources and can be obtained and stored by electrochemical reactions in suitable electrochemical devices. Fuel cells that convert the primary energy source, H_2, to the secondary one, electricity, to generate water (H_2O) are key technologies for a hydrogen economy. H_2 can be produced from H_2O as a huge storeroom of H_2, although a lot of electric energy is required in splitting H_2O into H_2 and oxygen (O_2) by electrolysis at conventional electrodes. In any event, electrochemistry, a truly interfacing science, plays vital and important role to construct environmentally clean, cheap, and sustainable energy systems.

Y. Kitazumi · K. Kano (✉)
Division of Applied Life Science, Graduate School of Agriculture, Kyoto University, Kyoto, Japan
e-mail: kitazumi.yuki.7u@kyoto-u.ac.jp; kano.kenji.5z@kyoto-u.ac.jp

M. Ishii, S. Wakai (eds.), *Electron-Based Bioscience and Biotechnology*,
https://doi.org/10.1007/978-981-15-4763-8_7

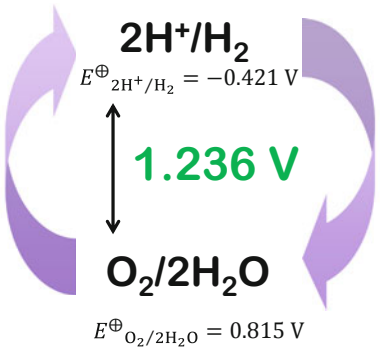

Fig. 7.1 Schematic of the hydrogen economy, in which two redox couples: $2H^+/H_2$ and $O_2/2H_2O$ play important roles. The difference in the biological standard redox potentials ($E^{\oplus}$) of the two couples is 1.236 V at 1×10^5 Pa and 25 °C. $E^{\oplus}$ is referred to the standard hydrogen electrode (SHE)

Future well-being of the planet Earth may lie in the hands of electrochemists (Rand 2011).

However, the electrochemical interconversions between proton (H^+) and H_2 and between O_2 and H_2O usually have large energy losses in kinetics at conventional electrodes. Such energy loss is often called overpotential in the field of electrochemistry. It is very important to minimize the energy loss during the interconversion of energy sources to realize ideal and sustainable energy systems. In order to decrease the overpotentials of the H_2 oxidation and the O_2 reduction in H_2/O_2 fuel cells, devices have to rely on the requirement of catalysts, usually novel metals such as platinum (Pt). Because of availability and economic issue in the use of Pt, extensive researches have been done during the last few decades to decrease or replace Pt in fuel cells. H_2O splitting into H_2 and O_2 also requires catalysts.

One of the strategies to decrease the overpotential of the interconversion is utilization of redox enzymes as electrode catalysts. Hydrogenase (H_2ase) catalyzes the reversible redox reactions of H^+/H_2, while multicopper oxidase (MCO) catalyzes a 4-electron redox reaction of O_2 without producing any intermediate. Photosynthetic organisms or thylakoid membranes can catalyze photochemical splitting of H_2O.

On one level, H_2 shows poor properties in storage and transportation issues. Alternative and attractive fuels in this sense may be some liquid or ionic solutes with high water solubility that can be completely burned in their oxidation. One of the possible fuels is formate ($HCOO^-$) (Asefa et al. 2019). However, it is very important to construct a technology to re-reduce its oxidized product, carbon dioxide (CO_2), in order to prevent an increase in the greenhouse gas. Unfortunately, the redox interconversion of the $CO_2/HCOO^-$ couple has extremely high kinetic barrier at conventional electrodes, and then large overpotentials are required. Energetic researches have been devoted to find and synthesize effective catalysts for the interconversion of the redox couple (Chaplin and Wragg 2003; Enthaler et al. 2010; Gunasekar et al. 2016; Asefa et al. 2019; Grubel et al. 2020). The platinum group elements show relatively high catalytic activity (Enthaler et al. 2010; Gunasekar et al. 2016; Grubel et al. 2020). However, the selectivity and activity in such metal-based catalytic reactions are not acceptable for ideal and sustainable energy systems. The

development of effective catalysts for the interconversion reaction is an attractive subject. From biochemical viewpoints, it is well-known that methylotrophic bacteria express a variety of redox enzymes involved in the C1 metabolism (Kletzin and Adams 1996; Rotaru et al. 2014; Shi et al. 2015). Molybdenum (Mo) or tungsten (W)-containing formate dehydrogenase (FDH) catalyzes the reversible interconversion of the $CO_2/HCOO^-$ redox couple under mild conditions (Reda et al. 2008; Bassegoda et al. 2014; Maia et al. 2016; Yu et al. 2017). Electrochemical properties of FDHs have been actively investigated (Reda et al. 2008; Bassegoda et al. 2014; Sakai et al. 2015, 2017; Jang et al. 2018; Jayathilake et al. 2019).

Significant advantageous properties of biological redox catalysts (or redox enzymes) compared with metal-based catalysts are (1) extremely high catalytic activity, (2) low reorganization energy, (3) high specificity, (4) high identicalness and uniformity (thanks to biological expression), and (5) enormous chemical versatility. These factors are very convenient from the viewpoint of their application. In addition, the redox potential of the electrochemically communicating site of redox enzymes can be definitely defined, which leads to more rigorous discussion on current-potential curves of catalytic waves. However, redox enzymes have huge size and are fragile. The size matter causes characteristic features in direct communication of enzymes with electrodes. In general, the non-catalytic direct redox signal density of redox enzymes is too low to be detected since the surface concentration of such enzymes with huge sizes is quite low, and therefore the enzymatically amplified catalytic redox signal is actually detectable. The orientation of redox enzymes is a key factor determining the distance between the electrode surface and the redox site located near the surface of the enzyme of a large size, since the standard interfacial electron transfer rate constant (k°) decreases exponentially with the distance (d) between the electrode surface and the redox site of the enzyme, as given by the following equation (Bard and Faulkner 2001):

$$k^\circ = k^\circ_{\max} \exp(-\beta d) \tag{7.1}$$

where $k^\circ_{\max}$ is the standard rate constant at the closest approach, and β is the decay coefficient. Therefore, it is very important to control the orientation of redox enzymes on electrodes by tuning the nanostructure and the surface property of mesoporous electrodes as scaffolds for the enzymes.

In this chapter, several applications of bioelectrocatalytic reactions of H_2ase and FDH will be introduced. The adsorption of these enzymes on suitably tuned mesoporous electrodes realizes bioelectrocatalytic reversible conversion of H_2 and HCOOH. MCO-modified electrodes and thylakoid membrane-modified electrodes realize a 4-electron reduction of O_2 and photobioelectrochemical splitting of H_2O, respectively. H_2/O_2 and $HCOO^-/O_2$ biofuel cells are constructed by the combination of suitable bioelectrodes. Photosynthetic energy conversion is also realized by the combination of these enzyme-modified electrodes.

7.2 H_2/O_2 Biofuel Cells

Biofuel cells (rightly, biological fuel cells) are bioelectrochemical devices that convert the reaction energy in the oxidation of several biological fuels with O_2 into the electrical energy with the aid of redox enzymes as electrode catalysts (Barton et al. 2004; Cracknell et al. 2008; Meredith and Minteer 2012; Mazurenko et al. 2017a, b; Mano and de Poulpiquet 2018). The concept of the biofuel cell was first introduced by Yahiro et al. (1964). Generally, biofuel cells consist of a two-electrode setup with the aid of corresponding redox enzymes (Fig. 7.2); fuels are oxidized at the bioanode, and electrons flow through the external electric circular to the biocathode, at which oxidants, usually O_2, are reduced (to H_2O). Some proton-exchange membrane is often employed to separate two compartments while accelerating H^+ transfer, although it is not essential thanks to the substrate specificity of redox enzymes. The first H_2/O_2 biofuel cell was reported in 2001 (Tsujimura et al. 2001a), though whole bacterial cells *Desulfovibrio vulgaris* (Hildenborough) were used as electrode catalysts. In the recent past, O_2-tolerant or O_2-sensitive H_2ases are frequently utilized as electrode catalysts in biocathodes of H_2/O_2 biofuel cells (Vincent et al. 2007; Armstrong and Hirst 2011; Lojou 2011; Mazurenko et al. 2017a, b).

H_2ases catalyze H_2 oxidation and also frequently inverse H^+ reduction. They are classified into [Ni–Fe]-, [Fe–Fe]-, and [Fe]-H_2ases according to the active site component (Vincent et al. 2007; Armstrong and Hirst 2011). The native electron acceptors of H_2ases can be replaced with several artificial redox compounds (in the oxidized form). Some redox compounds reduced by the H_2ase reaction are re-oxidized at electrodes. In this way, the enzymatic reaction can be coupled with the electrode reaction through the artificial redox compound called mediator. This reaction system is referred to as mediated electron transfer (MET)-type bioelectrocatalysis (Fig. 7.3, upper) and is applicable to most other redox enzymes.

Suitably tuned electrodes can play as electron donors for H_2ases; the enzyme reaction is directly coupled with the electrode reaction without any mediator. The reaction system is referred to as direct electron transfer (DET)-type bioelectrocatalysis (Fig. 7.3, lower). Enzymes capable of the DET-type reactions

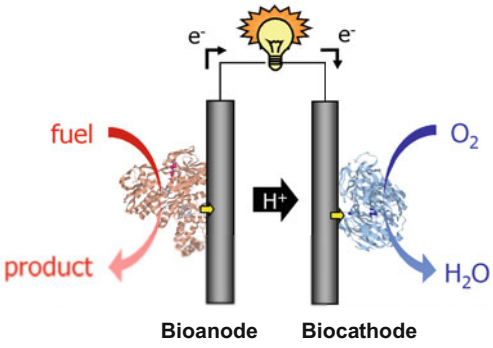

Fig. 7.2 Schematic of biofuel cells

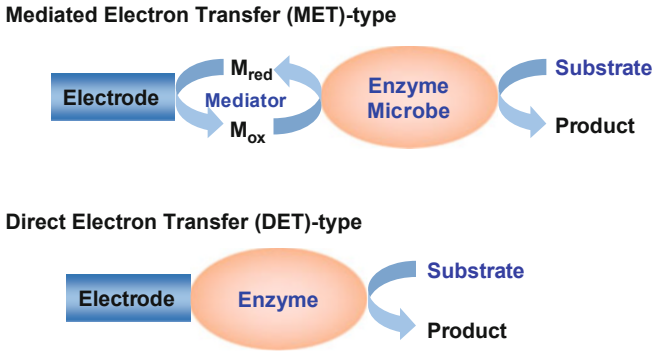

Fig. 7.3 Schematic of mediated electron transfer (MET) and direct electron transfer (DET)-type bioelectrocatalyses

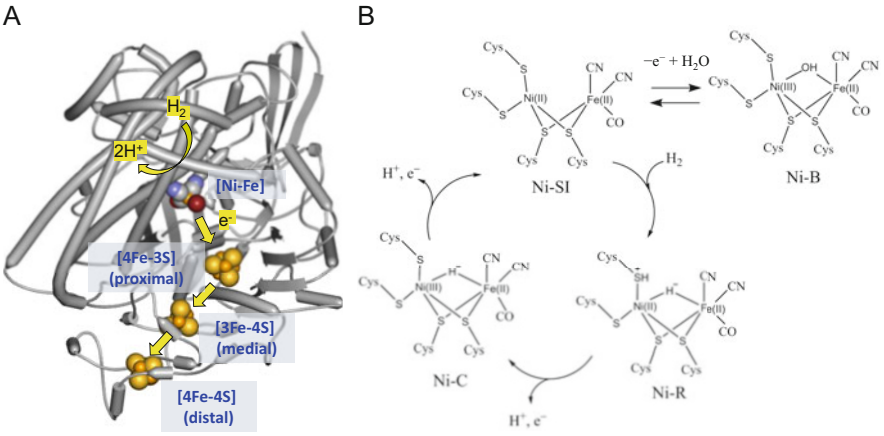

Fig. 7.4 (**a**) Structure of a [Ni–Fe]-H_2ase. The structural data were taken from PDB 5XLE. The pathway of the electron transfer is indicated by yellow arrow lines. (**b**) The structural change in the catalytic cycle and the oxidative inactivation to the Ni-B state (Mazurenko et al. 2017b)

are small in number. Standard and O_2-sensitive [Ni–Fe] H_2ase from *Desulfovibrio vulgaris* Miyazaki F (*Dv*MF) is composed of large and small subunits. The large subunit contains [Ni–Fe] cluster as the catalytic center for the $2H^+/H_2$ conversion, while the small subunit contains three iron-sulfur (FeS) clusters called proximal, medial, and distal in turn from the [Ni–Fe] cluster (Fig. 7.4). In the DET-type communication, the distal FeS cluster plays as the electrode-active redox center (Lojou 2011). [Ni–Fe]-H_2ases from *Dv*MF, *Escherichia coli* (*Ec*), *Allochromatium vinosum* (*Av*), *Ralstonia eutropha* (*Re*), and *Ralstonia metallidurans* (*Rm*) have been frequently used as bioanode catalysts for the H_2 oxidation (Mazurenko et al. 2017b), since the formal potential of the distal FeS cluster of these H_2ases is rather negative. This characteristic is important to minimize the overpotential of the H_2 oxidation.

Thermostable and O_2-tolerant H_2ase from *Hydrogenovibrio marinus* (*Hm*) (Yoon et al. 2011) is also useful, though its formal potential is slightly positive compared with those of the abovementioned H_2ases (So et al. 2016).

MCO catalyzes a 4-electron reduction of O_2 into H_2O without generation of intermediate species. The native electron donors of MCOs can be replaced with artificial redox compounds (reduced form) or even with electrodes. Therefore, MCO can play as an electrode catalysis in the 4-electron reduction of O_2 in both MET- and DET-type bioelectrocatalyses (Mano and de Poulpiquet 2018). MCOs contain four copper (Cu) atoms classified into a type 1 Cu site (T1) and a type 2–3 Cu (T2/3) cluster. O_2 is reduced at the T2/3 Cu cluster, while electrons are accepted at the T1 Cu site from reduced mediators in the MET-reaction or from electrodes in the DET-reaction (Fig. 7.5). Bilirubin oxidase (BOD) from the fungus *Myrothecium verrucaria* (*Mv*) has been frequently utilized as a bioelectrocatalysis, since *Mv* BOD works even at neutral pH (Tsujimura et al. 2004) (in contrast, optimum pH values of most MCOs are located in slightly acidic region), and the formal potential of the T1 Cu site is rather positive (Tsujimura et al. 2005; Christenson et al. 2006; Kamitaka et al. 2007). Thermostable BOD from the bacterium *Bacillus pumilus* (*Bp*) is also utilized (de Poulpiquet et al. 2014).

Electrochemical coupling of an H_2ase-based bioanode and an MCO-based biocathode yields an H_2/O_2 biofuel cell. The power density of fuel cells is the product of the current density and the cell voltage. In order to increase the limiting current density, mesoporous materials such as Ketjen black, carbon nanotubes, carbon nanofibers, and gold nanoparticles are often utilized, since the ratio of the electrochemically active surface area against the projected area increases, as the major reason in the MET-type reaction.

On the other hand, such mesoporous structures work as scaffolds suitable for the DET-type reaction and improve the heterogeneous electron transfer kinetics. Probability of the enzyme orientations suitable for the DET-reactions increases in the mesoporous structures with sizes close to that of the enzyme (Sugimoto et al. 2016, 2017; Kitazumi et al. 2020). This is the curvature effect of the mesoporous structure in the DET-type reaction. The microporous structure also improves the heterogeneous electron transfer kinetics between enzymes and the electrode because of an increase in the electric field at the edge of the microstructures due to the expansion of the electric diffuse double layer (Kitazumi et al. 2013, 2020).

On the other hand, in order to increase the open-circuit voltage (OCV) and to decrease the overpotential in H_2/O_2 biofuel cells, it is important to utilize an H_2ase with a negative formal potential for the distal FeS and an MCO with a positive formal potential for the T1 Cu site. Fast kinetics in the electroenzymatic reaction is also important to decrease the operational overpotential. The curvature effect and the electric double layer effect of nanostructured materials are very important to improve the performance of the DET-type bioelectrocatalysis. In the case of the MET-type reaction, some energy loss (some gap in the formal potentials of a mediator and an enzyme, $E_M^{\circ\prime}$ and $E_E^{\circ\prime}$) is required to create the standard driving force ($-\Delta_r G^\circ$) in the electron transfer from a substrate-reduced enzyme to an oxidized mediator for the

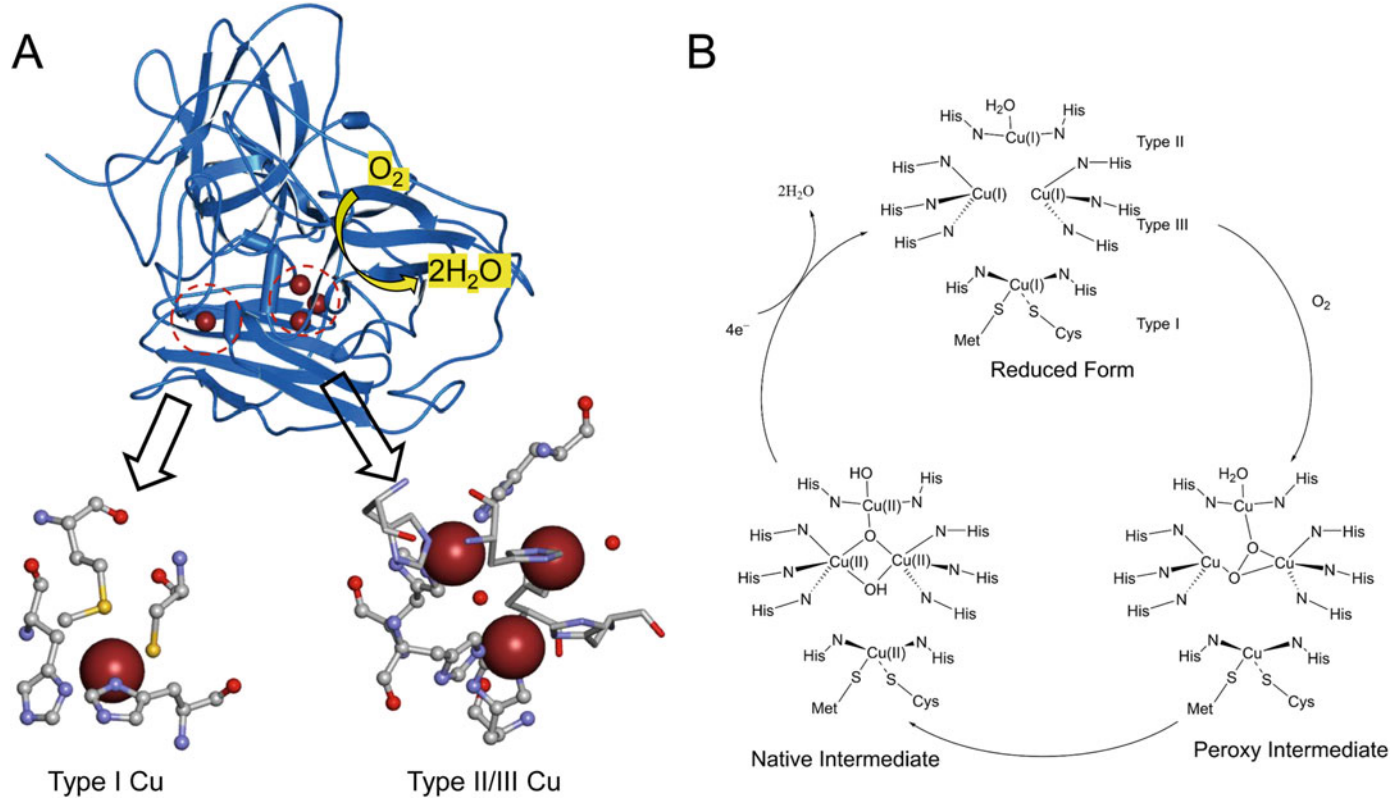

Fig. 7.5 (**a**) Structure of BOD. The structural data were taken from PDB 3ABG. (**b**) The catalytic cycle of a 4-electron reduction of O_2 at the T2/3 Cu site (Mazurenko et al. 2017b)

substrate oxidation (and vice versa), in which $\Delta_r G^\circ$ is the standard Gibbs energy of the reaction and is given by:

$$\Delta_r G^\circ = -nF\left(E_M^{\circ\prime} - E_E^{\circ\prime}\right), \tag{7.2}$$

where n and F are the total number of electrons in the electron transfer and the Faraday constant, respectively. The requirement of the situation in which $E_M^{\circ\prime} > E_E^{\circ\prime}$ for the substrate oxidation is attributable to the fact that the self-exchange electron transfer rate constant (k_{self}) of artificial mediators is usually very small (or the reorganization energy (λ) is usually very large for artificial mediators that easily change the structure during the redox reaction), as given by the following equations (Marcus and Sutin 1985):

$$k \cong \sqrt{k_{self,D} k_{self,A} \exp\left(-\frac{\Delta_r G^\circ}{RT}\right)}, \tag{7.3}$$

and

$$RT \ln \frac{k_{self}}{Z} = -\Delta^\ddagger G_{self}^\circ = -\frac{\lambda}{4}, \tag{7.4}$$

where $k_{self,\ D}$ and $k_{self,\ A}$ are k_{self} of the electron donor and acceptor, respectively. R and T are the gas constant and the absolute temperature, respectively. Z is a coefficient of the absolute kinetics, and $\Delta^\ddagger G_{self}^\circ$ is the standard Gibbs energy of the activation. In this sense, the DET-type bioelectrocatalysis is preferred to the MET-type one in theory to minimize the overpotential.

Since the saturated concentrations of H_2 and O_2 in aqueous solutions are very low, the catalytic current becomes controlled by the diffusion of the gaseous substrates soon after electrolysis under quiescent conditions. Gas bubbling is often utilized to convect the electrolyte solutions and supply such gaseous substrates. More suitable method to minimize or avoid the concentration polarization near bioelectrodes is utilization of gas diffusion bioelectrodes under quiescent conditions (Fig. 7.6). A review article details several setups of the systems (So et al. 2017). In order to bring out better performance of gas diffusion bioelectrodes, the control of the hydrophobicity for the gas diffusion and the hydrophilicity for the enzymatic reaction is very important. Some redox enzymes utilize gaseous substrates not in solvated state but in gas phase. Typical examples are Mo- or W-complexed molybdopterin FDHs (Zhong et al. 2015) and probably most of H_2ases. Therefore, the three-boundary phase in gas diffusion bioelectrodes provides a situation very suitable for the DET-type bioelectrocatalyses of gaseous substrates and drastically increases the catalytic current density.

Unfortunately, H_2ases have one drawback in electrochemical application; most of H_2ases including O_2-tolerant ones are non-catalytically oxidized and inactivated into the Ni-B state (Fig. 7.4) at high potentials of electrodes and solutions even in the

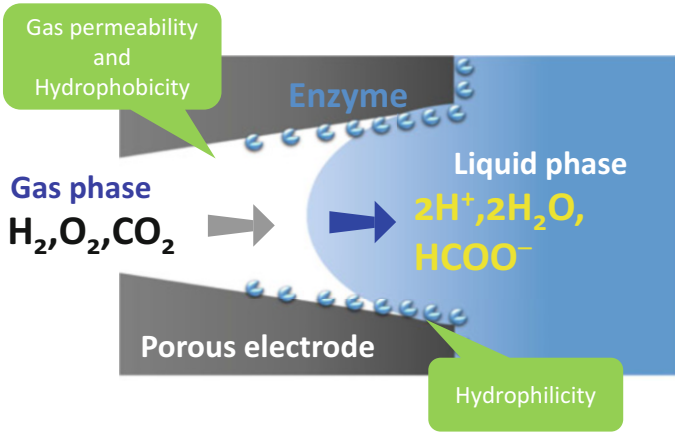

Fig. 7.6 Schematic of gas diffusion electrodes

absence of O_2. Although the oxidative inactivation is reversible, the characteristic restricts the performance of H_2/O_2 biofuel cells especially at decreased operational potentials, at which the electrode potential of the H_2ase-bioanode would become sufficiently positive. Several attempts have been reported in order to overcome this issue. In the MET-type configuration, hydrogels based on viologen entities were used to immobilize *Dv*MF H_2ase and mediate the electron transfer from the enzyme to the electrode (Plumeré et al. 2014). The enzymatically reduced redox gels on the electrode were auto-oxidized with dissolved O_2 on the side of the electrolyte solution, but the partially oxidized gels were immediately reduced by the MET-type enzymatic reaction, and then the solution potential in the gels remained rather negative, resulting in the protection of the O_2-sensitive H_2ase in the gels from the oxidative inactivation by O_2. Because of the MET-type reaction system, direct oxidative inactivation of H_2ase on the bioanode is also minimized. In the DET-type configuration, it was found that a gas diffusion electrode system was effective to protect the oxidative inhibition of H_2ase even at high electrode potentials (So et al. 2017). Since the oxidative inactivation at electrodes can be considered as an electrochemical competitive inhibition of H_2ase (So et al. 2014a, b) (Fig. 7.4), the inhibition was minimized by the catalytic cycle predominantly proceeding at increased concentrations of gaseous H_2 at the three-boundary phase biointerface.

The performance of H_2/O_2 biofuel cells is well summarized in the literature (Mazurenko et al. 2017b). The OCV values of most of the H_2/O_2 biofuel cells in the literature are approximately 1 V, and some DET-type electroenzymatic devices give OCVs of 1.12–1.14 V (Monsalve et al. 2015; So et al. 2016; Xia et al. 2016). These OCV values are very close to the standard electromotive force of 1.23 V for the 1 atm-H_2/O_2 fuel cell at 25 °C and OCVs of Pt-based polymer electrolyte H_2/O_2 fuel cells (about 1 V) at 80 °C. This means that the overpotentials in both of the

bioanode and biocathode are very small. The maximum power density of the H_2/O_2 biofuel cells reported to date is 6.1 mW cm^{-2} at 25 °C under 1 atm-H_2/air conditions (Xia et al. 2016) and 8.4 mW cm^{-2} at 40 °C under 1 atm-H_2/O_2 conditions (So et al. 2016) both under quiescent conditions. These values are the world record at present as H_2/O_2 biofuel cells.

7.3 Construction of Photobioelectrochemical H_2O Splitting System

Water splitting ($2H_2O \rightarrow 2H_2 + O_2$) would be one of the important technological breakthroughs to construct a hydrogen economy. Electrolysis of H_2O at conventional electrodes results in large overpotential (and then large energy loss), though water splitting of seawater (or sodium chloride solution) is industrially used to provide sodium hydroxide and chlorine. Photochemical water splitting is still under development. The photosynthesis of photosynthetic organisms occurs in the thylakoid membrane in the chloroplast. The photosynthesis converts CO_2 in the atmosphere to organic substances by excited electrons generated by photobiochemical splitting of H_2O as a sacrificial reagent (Barber 2009); in water splitting in the photosynthesis, the exited electrons are shunted, not to H^+, but to the electron transport chain in photosystem II (PSII). When the excited electrons are extracted to an electrode, the photosynthetic charge separation system may be regarded as a photo-driven bioanode. In order to construct photo-driven bioanodes, several artificial electron acceptors have been utilized for chloroplasts (Haehnel and Hochheimer 1979; Okano et al. 1984), photosystem I (PSI) (Hill et al. 1985), PSII (Lemieux et al. 2001), photosynthetic microorganisms (Martens and Hall 1994; Torimura et al. 2001; Tsujimura et al. 2001b), and thylakoid membranes (Mimcault and Carpentier 1989; Carpentier et al. 1989; Hasan et al. 2014).

Characteristics required as mediators to be used in photo-driven bioanodes are low barrier in electrode kinetics, high stability, suitable solubility, and low redox potential (to minimize the overpotential). In addition, ideal mediators should have large O_2 tolerance (because O_2 evolution occurs at the bioanode with the PSII function) and have high permeability of biomembranes when whole cells or organisms are used. By considering these factors and a linear-free energy relationship in the electron transfer from thylakoid membranes to mediators (Kano 2019), our group proposed to use 1,2-naphthoquinone (NQ) or hexaammineruthenium (III) ($[Ru(NH_3)_6]^{3+}$) as a mediator of photo-driven bioanodes based on thylakoid membranes from spinach (Takeuchi et al. 2018; Adachi et al. 2019). The thylakoid membranes were embedded within water-spread multi-walled carbon nanotubes (MWCNTs) that were mounted on a light-permeable indium tin oxide (ITO) electrode (Fig. 7.7). MWCNTs are stabilized with each other by π–π staking after drying. ITO electrodes were spattered to form a thin gold (Au) film with a thickness of 4 nm before

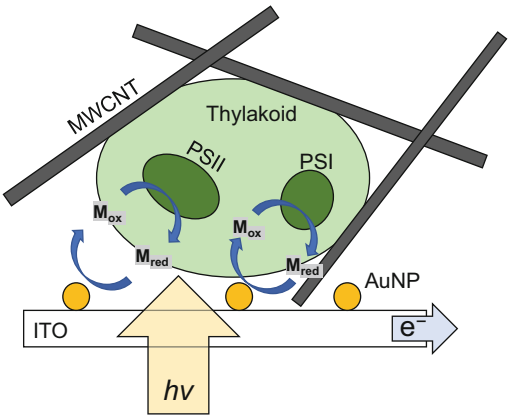

Fig. 7.7 Schematic of a thylakoid membrane/MWCNT-mounted Au/ITO electrode as a photo-driven bioanode

MWCNT-mounting in order to improve the electrode kinetics of the mediator. The thin Au film was acceptably light permeable. The photocurrent densities were 0.1 mA cm^{-2} with NQ (Takeuchi et al. 2018) and 0.18 mA cm^{-2} with $[Ru(NH_3)_6]^{3+}$ (Adachi et al. 2019) at a light flux density of 1.5 mmol m^{-2} s^{-1}. The latter value of the photo current density is the world record at present as a photo-driven bioanode to realize photobioelectrochemical H_2O splitting.

Electrochemical coupling of the photo-driven bioanode with a DET-type MCO-based biocathode yielded a bioelectrochemical photocell (called bio-solar cell) (Adachi et al. 2019). The cell exhibited an OCV of 0.61 V and a maximum power of 50 μW cm^{-2}, the best performance in the world. Ideally, in this bio-solar cell, O_2 is reduced to H_2O at the biocathode and is regenerated at the photo-driven bioanode with PSII from H_2O. This is a typical and ideal example of an electrochemical device to underpin a hydrogen economy in Fig. 7.1, though further trial to decrease the overpotential of the photobioelectrochemical H_2O splitting is required in the future.

7.4 Bioelectrochemical Hydrogen Economy and Its Expansion to C1 Society

As mentioned in Sect. 7.2, most H_2ases catalyze both H_2 oxidation and H^+ reduction. The broken line in Fig. 7.8 shows a typical steady-state catalytic wave of bidirectional DET-type bioelectrocatalysis in the case of a system with a low kinetic barrier in the interfacial electron transfer between an enzyme and an electrode (Armstrong and Hirst 2011). The oxidized and reduced substrates are reversibly interconverted, indicating that the system does not have any overpotential in the interconversion. Such reversible redox reactions are almost impossible to be realized with metal-based catalysts and are only realized by biocatalysts in electrochemistry.

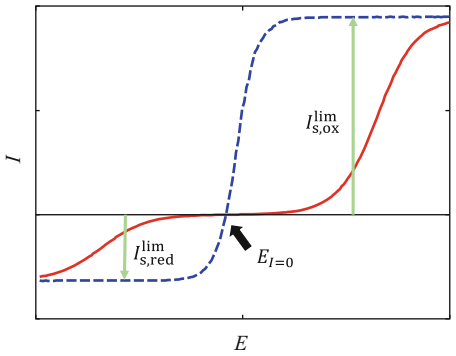

Fig. 7.8 Conceptional steady-state catalytic waves in bidirectional DET-type bioelectrocatalysis under quiescent conditions with rather large (broken line) and small (solid line) values of the standard interfacial electron transfer rate constant (k°)

Similar sigmoidal waves of bidirectional DET-type bioelectrocatalysis were observed with W-containing FDH from *Methylobacterium extorquens* (*Me*) AM1 for two redox couples of CO_2/$HCOO^-$ and NAD^+/NADH (Sakai et al. 2017; Reda et al. 2008; Bassegoda et al. 2014) and ferredoxin-$NADP^+$ reductase (FNR) from *Chlamydomonas reinhardtii* for a redox couple of $NADP^+$/NADPH (Siritanaratkul et al. 2017; Wan et al. 2018).

The FDH from *Me*AM1 is a heterodimeric soluble enzyme in the family of molybdopterin enzyme; W-containing subunit contains a tungstopterin cofactor as the catalytic center for the CO_2/$HCOO^-$ interconversion and FeS clusters, while diaphorase subunit contains a non-covalently bound flavin mononucleotide (FMN) as the catalytic center for the NAD^+/NADH interconversion and FeS clusters (Fig. 7.9). The FNR is a monomeric flavoenzyme with a molecular mass of 45 kDa having flavin adenine dinucleotide (FAD) as a sole redox cofactor.

The appearance of the steady-state wave indicates that any concentration polarization does not occur at the electrode surface and that the current is controlled by the electroenzymatic process. At positive potentials, the steady-state current reaches a limiting value ($I^{lim}_{s,ox}$) for the oxidation of a reduced substrate (H_2 in the case of H_2ase) as given by:

$$I^{lim}_{s,ox} = n_S F A k_{c,ox} \Gamma_E, \tag{7.5}$$

where n_S is the number of electrons of the substrate, A is the surface area of the electrode, $k_{c,\,ox}$ is the catalytic constant of the substrate oxidation by the enzyme, and Γ_E is the surface concentration of the enzyme. At negative potentials, the steady-state current reaches a limiting value ($I^{lim}_{s,red}$) for the reduction of an oxidized substrate (H^+ in the case of H_2ase) as given by:

$$I^{lim}_{s,red} = n_S F A k_{c,red} \Gamma_E, \tag{7.6}$$

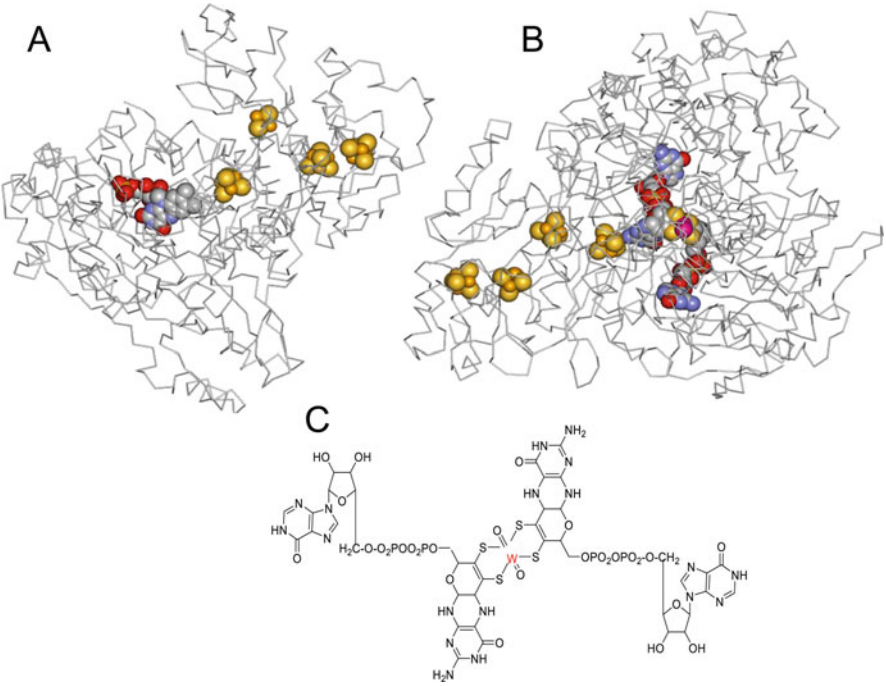

Fig. 7.9 Tentative structures of (**a**) diaphorase subunit and (**b**) molybdopterin subunit. (**c**) The structure of W-centered molybdopterin (Moco). The structural data for diaphorase and molybdopterin subunits were taken from PDB 5XF9 (NAD^+-reducing H_2ase) and PDB 1H0H (formate dehydrogenase from *Desulfovibrio gigas*), respectively

where $k_{c,red}$ is the catalytic constant of the substrate reduction. The ratio $I_{s,ox}^{lim}/I_{s,red}^{lim}(=k_{c,ox}/k_{c,red})$ does not necessarily correspond to the equilibrium potential of the substrate ($E_{S,\ eq}$):

$$E_{S,eq} = E_S^{\circ\prime} + \frac{n_S F}{RT} \ln \frac{c_{ox}}{c_{red}}, \tag{7.7}$$

where $E_S^{\circ\prime}$ is the formal potential of the substrate, and c_{ox} and c_{red} are the bulk concentrations of the oxidized and reduced substrates, respectively. The reason is that the process is not an elementary reaction, and therefore low of mass action does not hold. Fortunately, the potential at which the steady-state sigmoidal wave crosses the potential axis of zero current (called zero current potential, $E_{I\ =\ 0}$) is identical with $E_{S,eq}$.

With a high kinetic barrier in the electron transfer between an enzyme and an electrode, steady-state waves show two sigmoidal parts, as shown by a solid line in Fig. 7.8. In such cases, one could not get the information on $E_{S,eq}$. The shifted values of the wave in the direction of the potential axis correspond to the overpotentials caused by the kinetic processes. When the catalytic constants are sufficiently large,

some concentration polarization will occur, and the current depends on time. Under such conditions, rotating disk electrode methods are required to get steady-state currents. When the limiting current is controlled by the diffusion of substrate, the reductive and oxidative limiting currents reflect c_{ox} and c_{red}, respectively, as in the case of non-catalytic conventional electrochemical measurements.

Even for the MET-type bioelectrocatalysis, bidirectional mono-sigmoidal waves were observed under logically tuned conditions for the $2H^+/H_2$ redox couple with *Desulfovibrio vulgaris* cells (Tatsumi et al. 1999) and the $CO_2/HCOO^-$ redox couple with W-containing FDH (Sakai et al. 2015).

The essential requirement for such a two-way DET-reaction is that $E_S^{\circ\prime}$ and the formal potential of the electrochemically active site in enzymes ($E_E^{\circ\prime}$) are close with each other in order to minimize the kinetic barrier of uphill intramolecular electron transfer of one of the bidirectional reactions in the enzymes, as evidenced by Eqs. (7.2) and (7.3), where $E_M^{\circ\prime}$ in Eq. (7.2) is replaced with $E_S^{\circ\prime}$. In the case of the MET reaction, it is very important to adjust the pH value to satisfy the condition in which $E_M^{\circ\prime} \cong E_E^{\circ\prime}$ (Tatsumi et al. 1999; Sakai et al. 2015).

The other requirement for fast electron transfer of the uphill reactions ($\Delta_r G^\circ > 0$) is that k_{self} in Eq. (7.3) should be very large, that is, λ in Eq. (7.4) should be very small. Peptide matrix frequently plays an important role to minimize the geometric change. Therefore, the uphill electron transfer is often observed in the intramolecular electron transfers in redox proteins in some instances. (Such situation of small value of λ in redox proteins also affects $E_E^{\circ\prime}$. For example, although Cu^+ prefers a tetrahedral coordination and the ligand of Cu^{2+} arranges in a square planar configuration, the ligands and the conformations of type I copper of blue copper proteins (e.g., of MCO) remain almost unchanged during the redox reaction, and they considerably deviate from those preferred by Cu^{2+}, leading to a destabilization of the oxidized state and then a rise in the formal potential to get strong oxidation activity.)

In the case of FDH, the formal potentials of tungstopterin, FeSs, and FMN seem to be located close with each other and also close with those of the redox couples of $CO_2/HCOO^-$ and $NAD(P)^+/NAD(P)H$. Molybdopterin enzymes frequently show the catalytic activity toward bidirectional redox reactions of biologically important redox couples with negative formal potentials such as the carboxylate/aldehyde redox couple (Reda et al. 2008; Bassegoda et al. 2014; Sakai et al. 2015; Huber et al. 1995; Siritanaratkul et al. 2017; Wan et al. 2018). Therefore, bioelectrocatalytic reactions with molybdopterin enzymes as well as H_2ases will attract lots of attention in the near future.

As mentioned above, H_2 is an attractive energy source in the sustainable society. Although H_2 has many excellent properties as fuel, H_2 has critical problems in its storage and transportation issues because of its gaseous properties. Liquid fuels or highly water-soluble ionic solutes are easy to store and transport. One of the possible candidates as fuels is $HCOO^-$ (Enthaler et al. 2010; Asefa et al. 2019) as described in Introduction. Since the formal potential of $CO_2/HCOO^-$ and H^+/H_2 is very close

with each other, the interconversion between the two redox couples is very useful to underpin the sustainable society:

$$CO_2 + H_2 \rightleftarrows HCOO^- + H^+ \tag{7.8}$$

Several attempts have been tried (Enthaler et al. 2010; Asefa et al. 2019). We have realized the reversible interconversion without overpotentials by using the bidirectional catalytic reactions of H_2ase from *Dv*MF and FDH from *Me*AM1 (Adachi et al. 2018). Such biotechnology would facilitate the storage and the transportation of the primary energy sources.

In addition, FDH from *Me*AM1 realizes the reversible interconversion between CO_2/$HCOO^-$ and NAD(P)$^+$/NAD(P)H couples:

$$CO_2 + NAD(P)H \rightleftarrows HCOO^- + NAD(P)^+ \tag{7.9}$$

On the other hand, NAD$^+$-reducing H_2ase (from *Hydrogenophilus thermoluteolus*) realizes the reversible interconversion between $2H^+$/H_2 and NAD(P)$^+$/NAD(P)H couples:

$$2H^+ + NAD(P)H \rightleftarrows H_2 + NAD(P)^+ + H^+ \tag{7.10}$$

The structure of the NAD$^+$-reducing H_2ase has been solved (Shomura et al. 2017) and is considered to be similar to that of the FDH from *Me*AM1.

7.5 Conclusion

Bioelectrochemical coupling of H_2ase and FDH reactions with the electrode reaction realizes electrochemically reversible redox reactions of the two redox couples, $2H^+$/H_2 and CO_2/$HCOO^-$, respectively. The redox couples are also reversibly interconverted with each other by using corresponding enzymes. NAD$^+$-reducing H_2ase, FDH, and FNR are also utilized as electrocatalysts for an electrochemically reversible redox reaction of the biologically most important redox couple, NAD(P)$^+$/NAD(P)H. Bioelectrocatalytic reactions based on MCO and thylakoid membrane realize the 4-electron reduction of O_2 and the photobioelectrochemical H_2O splitting, respectively, with small overpotentials. These bioelectrochemical and biochemical reactions can construct a hydrogen/C1 economy as an expansion of the hydrogen economy (Fig. 7.10).

In addition, the NAD(P)$^+$/NAD(P)H redox couple can be reversibly linked to the redox couples $2H^+$/H_2 and CO_2/$HCOO^-$ by NAD$^+$-reducing H_2ase and FDH, respectively. The reversible NAD(P)$^+$/NAD(P)H redox couple is also linked to a huge variety of biological redox reactions by NAD(P)-dependent dehydrogenases. This linkage is very useful in (electro)enzymatic organic synthesis and

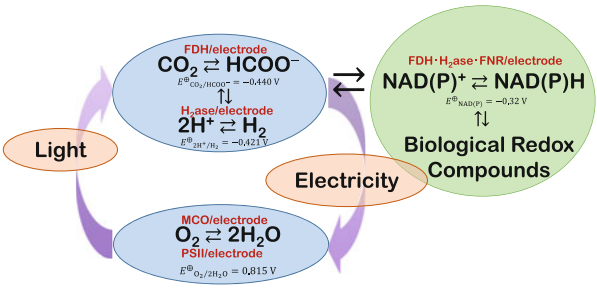

Fig. 7.10 Schematic of a bioelectrochemical/biochemical hydrogen/C1 economy. $E^{\oplus}$ is the biological standard redox potential vs. SHE

bioelectrochemical sensing. The proposed hydrogen/C1 economy is indeed an environmentally clean, cheap, and sustainable energy system.

References

Abe JO, Popoola API, Ajenifuja E, Popoola OM (2019) Hydrogen energy, economy and storage: review and recommendation. Int J Hydrog Energy 44:15072–15086

Adachi T, Kitazumi Y, Shirai O, Kano K (2018) Construction of a bioelectrochemical formate generating system from carbon dioxide and dihydrogen. Electrochem Commun 97:78–76

Adachi T, Kataoka K, Kitazumi Y, Shirai O, Kenji Kano K (2019) A bio-solar cell with thylakoid membranes and bilirubin oxidase. Chem Lett 48:686–689

Armstrong FA, Hirst J (2011) Reversibility and efficiency in electrocatalytic energy conversion and lessons from enzymes. Proc Natl Acad Sci U S A 108:14049–14054

Asefa T, Koh K, Yoon CW (2019) CO_2-mediated H_2 storage-release with nanostructured catalysis: recent progress, challenges, and perspectives. Adv Energy Mater 9:1901158

Barber J (2009) Photosynthetic energy conversion: natural and artificial. Chem Soc Rev 38:185–196

Bard AJ, Faulkner LR (2001) Electrochemical methods fundamentals and applications, 2nd edn. Wiley, New York, pp 130–132, Section 3.6.4

Barton SC, Gallaway J, Atanassov P (2004) Enzymatic biofuel cells for implantable and microscale devices. Chem Rev 104:4867–4886

Bassegoda A, Madden C, Wakerley DW, Reisner E, Hirst J (2014) Reversible interconversion of CO_2 and formate by a molybdenum-containing formate dehydrogenase. J Am Chem Soc 136:15473–15476

Carpentier R, Lemieux S, Mimeault M, Purcell M, Goetze DC (1989) A photoelectrochemical cell using immobilized photosynthetic membranes. J Electroanal Chem 276:391–401

Chaplin RPS, Wragg AA (2003) Effects of process conditions and electrode material on reaction pathways for carbon dioxide electroreduction with particular reference to formate formation. J Appl Electrochem 33:1107–1123

Christenson A, Shleev S, Mano N, Heller A, Gorton L (2006) Redox potentials of the blue active sites of bilirubin oxidases. Biochim Biophys Acta Bioenerg 1757:1634–1641

Cracknell JA, Vincent KA, Armstrong FA (2008) Enzymes as working or inspirational electrocatalysts for fuel cells and electrolysis. Chem Rev 108:2439–2461

de Poulpiquet A, Ciaccafava A, Gadiou R, Gounel S, Giudici-Orticoni MT, Mano N, Lojou E (2014) Design of a H_2/O_2 biofuel cell based on thermostable enzymes. Electrochem Commun 42:72–74

Enthaler S, von Langermann J, Schmidt T (2010) Carbon dioxide and formic acid—the couple for environmental-friendly hydrogen storage? Energy Environ Sci 3:1207–1217

European Commission (2003) Hydrogen energy and fuel cells: a vision of our future. Office for Official Publications of the European Communities, Luxembourg

Grubel K, Jeong H, Yoon CW, Autrey T (2020) Challenges and opportunities for using formate to store, transport, and use hydrogen. J Energy Chem 41:216–224

Gunasekar GH, Park K, Jung K-D, Yoon S (2016) Recent developments in the catalytic hydrogenation of CO_2 to formic acid/formate using heterogeneous catalysts. Inorg Chem Front 3:882–895

Haehnel W, Hochheimer HJ (1979) On the current generated by a galvanic cell driven by photosynthetic electron transport. Bioelectrochem Bioenerg 6:563–574

Hasan K, Dilgin Y, Emek SC, Tavahodi M, Akerlund HE, Albertsson P, Gorton L (2014) Photoelectrochemical communication between thylakoid membranes and gold electrodes through different quinone derivatives. ChemElectroChem 1:131–139

Hill HAO, Walton NJ, Whitford D (1985) The coupling of heterogeneous electron transfer to photosystem-1. J Electroanal Chem 187:109–119

Huber C, Skopan H, Feicht R, White H, Simon H (1995) Pterin cofactor, substrate specificity, and observations on the kinetics of the reversible tungsten-containing aldehyde oxidoreductase from *Clostridium thermoaceticum*. Arch Microbiol 164:110–118

Jang J, Jeon BW, Kim YH (2018) Bioelectrochemical conversion of CO_2 to value added product formate using engineered *Methylobacterium extorquens*. Sci Rep 8:7211

Jayathilake BS, Bhattachrya S, Vaidehi N, Narayanan SR (2019) Efficient and selective electrochemically driven enzyme-catalyzed reduction of carbon dioxide to formate using formate dehydrogenase and an artificial cofactor. Acc Chem Res 52:676–685

Kamitaka Y, Tsujimura S, Kataoka K, Sakurai T, Ikeda T, Kano K (2007) Effects of axial ligand mutation of the type I copper site in bilirubin oxidase on direct electron transfer-type bioelectrocatalytic reduction of dioxygen. J Electroanal Chem 601:119–124

Kano K (2019) Fundamentals and applications of redox enzyme-functionalized electrode reactions. Electrochemistry 87:301–311

Kitazumi Y, Shirai O, Yamamoto M, Kano K (2013) Numerical simulation on diffuse double layer around microporous electrodes based on Poisson-Boltzmann equation. Electrochim Acta 112:171–175

Kitazumi Y, Shirai O, Kano K (2020) Significance of nanostructures of an electrode surface in direct electron transfer-type bioelectrocatalysis of redox enzymes, Chap. 7. In: Lakhveer Singh L, Mahapatra DM, Liu H (eds) ACS symposium series 1342 "Novel catalyst materials for bioelectrochemical systems: fundamentals and applications". American Chemical Society, Washington, DC, pp 147–163

Kletzin A, Adams MWW (1996) Tungsten in biological systems. FEMS Microbiol Rev 18:5–63

Lemieux S, Carpentier R, Allen H, Hill O, Walton NJ, Whitford D (2001) Properties of a photosystem II preparation in a photochemical cell. J Electroanal Chem 496:109–119

Lojou E (2011) Hydrogenases as catalysts for fuel cells: strategies for efficient immobilization at electrode interfaces. Electrochim Acta 56:10385–10397

Maia LB, Fonseca L, Moura I, Moura JJG (2016) Reduction of carbon dioxide by a molybdenum-containing formate dehydrogenase: a kinetic and mechanistic study. J Am Chem Soc 138:8834–8846

Mano N, de Poulpiquet A (2018) O_2 reduction in enzymatic biofuel cells. Chem Rev 118:2392–2468

Marcus RA, Sutin N (1985) Electron transfers in chemistry and biology. Biochim Biophys Acta 811:265–322

Martens N, Hall EAH (1994) Diaminodurene as a mediator of a photocurrent using intact cells of cyanobacteria. Photochem Photobiol 59:91–98

Mazurenko I, de Poulpiquet A, Lojou E (2017a) Recent developments in high surface area bioelectrodes for enzymatic fuel cells. Curr Opin Electrochem 5:74–84

Mazurenko I, Wang X, de Poulpiquet A, Lojou E (2017b) H_2/O_2 enzymatic fuel cells: from proof-of-concept to powerful devices. Sustain Energy Fuels 1:1475–1501

Meredith MT, Minteer SD (2012) Biofuel cells; enhanced enzymatic bioelectrocatalysis. Annu Rev Anal Chem 5:157–179

Mimcault M, Carpentier R (1989) Kinetics of photocurrent induction by a thylakoid containing electrochemical cell. J Electroanal Chem 276:145–158

Monsalve K, Mazurenko I, Lalaoui N, Le Goff A, Holzinger M, Infossi P, Nitsche S, Lojou JY, Giudici-Orticoni MT, Cosnier S, Logou E (2015) A H_2/O_2 enzymatic fuel cell as a sustainable power for a wireless device. Electrochem Commun 60:216–220

Okano M, Iida T, Shinohara H, Kobayashi H (1984) Water photolysis by a photoelectrochemical cell using an immobilized chloroplasts-methyl viologen system. Agric Biol Chem 48:1977–1983

Plumeré N, Rüdiger O, Oughli A, Williams R, Vivekananthan J, Pöller S, Lubitz W, Shuhmann W (2014) A redox hydrogel protects hydrogenase from high-potential deactivation and oxygen damage. Nat Chem 6:822–827

Rand DAJ (2011) A journey on the electrochemical road to sustainability. J Solid State Electrochem 15:1579–1622

Reda T, Plugge CM, Abram NJ, Hirst J (2008) Reversible interconversion of carbon dioxide and formate by an electroactive enzyme. Proc Natl Acad Sci U S A 105:10654–10658

Ren JW, Musyoka NM, Langmi HW, Mathe M, Liao SL (2017) Current research trends and perspectives on materials-based hydrogen storage solution: a critical review. Int J Hydrog Energy 42:289–311

Rotaru A-E, Shrestha PM, Liu F, Shrestha M, Shrestha D, Embree M, Zengler K, Wardman C, Nevin KP, Lovley DR (2014) A new model for electron flow during anaerobic digestion: direct interspecies electron transfer to *Methanosaeta* for the reduction of carbon dioxide to methane. Energy Environ Sci 7:408–415

Sahaym U, Norton MG (2008) Advances in the application of nanotechnology in enabling a 'hydrogen economy'. J Mater Sci 43:5395–5429

Sakai K, Hsieh BC, Maruyama A, Kitazumi Y, Shirai O, Kano K (2015) Interconversion between formate and hydrogen carbonate by tungsten-containing formate dehydrogenase-catalyzed mediated bioelectrocatalysis. Sens Biosens Res 5:90–96

Sakai K, Sugimoto Y, Kitazumi Y, Shirai O, Takagi K, Kano K (2017) Direct electron transfer-type bioelectrocatalytic interconversion of carbon dioxide/formate and NAD^+/NADH redox couples with tungsten-containing formate dehydrogenase. Electrochim Acta 228:537–544

Shi J, Jiang Y, Jiang Z, Wang X, Wang X, Zhang S, Han P, Yang C (2015) Enzymatic conversion of carbon dioxide. Chem Soc Rev 44:5981–6000

Shomura Y, Taketa M, Nakashima H, Tai H, Nakagawa H, Ikeda Y, Ishii M, Igarashi Y, Nishihara H, Yoon KS, Ogo S, Hirota S, Higuch Y (2017) Structural basis of the redox switches in the NAD^+-reducing soluble [NiFe]-hydrogenase. Science 357:928–938

Siritanaratkul B, Megarity CF, Roberts TG, Samuels TOM, Winkler M, Warner JH, Happe T, Armstrong FA (2017) Transfer of photosynthetic $NADP^+$/NADPH recycling activity to a porous metal oxide for highly specific, electrochemically-driven organic synthesis. Chem Sci 8:4579–4586

So K, Kitazumi Y, Shirai O, Kurita K, Nishihara H, Higuchi Y, Kano K (2014a) Gas-diffusion and direct electron transfer-type bioanode for hydrogen oxidation with oxygen-tolerant [NiFe]-hydrogenase as an electrocatalyst. Chem Lett 43:1575–1577

So K, Kitazumi Y, Shirai O, Kurita K, Nishihara H, Higuchi Y, Kano K (2014b) Kinetic analysis of inactivation and enzyme reaction of oxygen-tolerant [NiFe]-Hydrogenase at direct electron transfer-type bioanode. Bull Chem Soc Jpn 87:1177–1185

So K, Kitazumi Y, Shirai O, Nishikawa K, Higuchi Y, Kano K (2016) Direct electron transfer-type dual gas diffusion H_2/O_2 biofuel cells. J Mater Chem A 4:8742–8749

So K, Sakai K, Kano K (2017) Gas diffusion bioelectrodes. Curr Opin Electrochem 5:173–182

Sugimoto Y, Takeuchi R, Kitazumi Y, Shirai O, Kano K (2016) Significance of mesoporous electrodes for noncatalytic faradaic process of randomly oriented redox proteins. J Phys Chem C 120:26270–26277

Sugimoto Y, Kitazumi Y, Shirai O, Kano K (2017) Effects of mesoporous structures on direct electron transfer-type bioelectrocatalysis: facts and simulation on a three-dimensional model of random orientation of enzymes. Electrochemistry 85:82–87

Takeuchi R, Suzuki A, Sakai K, Kitazumi Y, Shirai O, Kano K (2018) Construction of photo-driven bioanodes using thylakoid membranes and multi-walled carbon nanotubes. Bioelectrochemistry 122:158–163

Tatsumi H, Takagi K, Fujita M, Kano K, Ikeda T (1999) Electrochemical study of reversible hydrogenase reaction of *Desulfovibrio vulgaris* cells with methyl viologen as an electron carrier. Anal Chem 71:1753–1759

Torimura M, Miki A, Wadano A, Kano K, Ikeda T (2001) Electrochemical investigation of *Cyanobacteria Synechococcus* sp. PCC7942-catalyzed photoreduction of exogenous quinones and photoelectrochemical oxidation of water. J Electroanal Chem 496:21–28

Tsujimura S, Fujita F, Tatsumi H, Kano K, Ikeda T (2001a) Bioelectrocatalysis-based dihydrogen/dioxygen fuel cell operating at physiological pH. Phys Chem Chem Phys 3:1331–1335

Tsujimura S, Wadano A, Kano K, Ikeda T (2001b) Photosynthetic bioelectrochemical cell utilizing cyanobacteria and water-generating oxidase. Enzyme Microb Technol 29:225–231

Tsujimura S, Nakagawa T, Kano K, Ikeda T (2004) Kinetic study of direct bioelectrocatalysis of dioxygen reduction with bilirubin oxidase at carbon electrodes. Electrochemistry 72:437–439

Tsujimura S, Kuriyama A, Fujieda N, Kano K, Ikeda T (2005) Mediated spectroelectrochemical titration of proteins for redox potential measurements by a separator-less one-compartment bulk electrolysis method. Anal Biochem 337:325–331

Vincent KA, Parkin A, Armstrong FA (2007) Investigating and exploiting the electrocatalytic properties of hydrogenases. Chem Rev 107:4366–4413

Wan L, Megarity CF, Siritanaratkul B, Armstrong FA (2018) A hydrogen fuel cell for rapid, enzyme-catalysed organic synthesis with continuous monitoring. Chem Commun 54:972–975

Xia HQ, So K, Kitazumi Y, Shirai Y, Nishikawa K, Higuchi Y, Kano K (2016) Dual gas-diffusion membrane- and mediatorless dihydrogen/air-breathing biofuel cell operating at room temperature. J Power Sources 335:105–112

Yahiro AT, Lee SM, Kimble DO (1964) Bioelectrochemistry: I. Enzyme utilizing bio-fuel cell studies. Biochim Biophys Acta 88:375–383

Yoon KS, Fukuda K, Fujisawa K, Nishihara H (2011) Purification and characterization of a highly thermostable, oxygen-resistant, respiratory [FeNi]-hydrogenase from marine, aerobic, hydrogen-oxidizing bacterium *Hydrogenovibrio marinus*. Int J Hydrog Energy 36:7081–7088

Yu X, Niks D, Mulchandani A, Hille R (2017) Efficient reduction of CO_2 by the molybdenum-containing formate dehydrogenase from *Cupriavidus necator* (*Ralstonia eutropha*). J Biol Chem 292:16872–16879

Zhong H, Fujii K, Nakano Y, Jin FM (2015) Effect of CO_2 bubbling into aqueous solutions used for electrochemical reduction of CO_2 for energy conversion and storage. J Phys Chem 119:55–61